


 Cite this: *RSC Adv.*, 2023, 13, 28089

# Homoleptic octahedral Co<sup>II</sup> complexes as precatalysts for regioselective hydroboration of alkenes with high turnover frequencies†

 Guoqi Zhang,<sup>a</sup> Haisu Zeng,<sup>ab</sup> Nora Zadori,<sup>a</sup> Camila Marino,<sup>a</sup> Shengping Zheng<sup>b</sup> and Michelle C. Neary<sup>b</sup>

Homoleptic complexes adopting octahedral coordination modes are usually less active in catalysis due to the saturated coordination around metal centers that prevents substrate activation in a catalytic event. In this work, we demonstrated that a homoleptic octahedral cobalt complex (**1**) of 4'-pyridyl-2,2':6',2''-terpyridine that experienced monoprotonation at the non-coordinating pyridyl moiety upon crystallization could serve as a highly efficient precatalyst for the hydroboration of styrene derivatives with Markovnikov selectivity. The solid-state structure of this precatalyst along with relevant homoleptic Co<sup>II</sup> and Fe<sup>II</sup> complexes has been characterized by X-ray crystallography. In the solid state, **1** features one-dimensional hydrogen-bonded chains that are further stacked by interchain  $\pi\cdots\pi$  interactions. The newly synthesized complexes (**1–3**) along with several known analogues (**4–6**) were examined as precatalysts for the hydroboration of alkenes. The best-performing system, **1**/KO<sup>t</sup>Bu was found to promote Markovnikov hydroboration of substituted styrenes with high turnover frequencies (TOFs) up to  $\sim 47\,000\text{ h}^{-1}$ , comparable to the most efficient polymeric catalyst [Co(pytpy)Cl<sub>2</sub>]<sub>n</sub> reported to date. Although some limitations in substrate scope as well as functional group tolerance exist, the catalyst shows good promise for several relevant hydrofunctionalization reactions.

 Received 8th September 2023  
 Accepted 15th September 2023

DOI: 10.1039/d3ra06113b

[rsc.li/rsc-advances](https://rsc.li/rsc-advances)

## Introduction

Hydrofunctionalization of unsaturated bonds provides a powerful tool for incorporating valuable functional groups into hydrocarbon compounds.<sup>1</sup> In particular, alkene hydroboration is one of the most popular and convenient ways to approach alkylboronates that have extensive applications in C–C bond forming processes through cross-coupling reactions.<sup>2</sup> Great advances have been made in the past decade toward developing metal-based catalysts utilizing various transition metals from precious Ru, Rh and Ir to earth abundant ones such as Fe, Co, Ni, Cu, and Mn,<sup>3–7</sup> with the latter being the focus of recent research as nowadays chemists are seeking lower cost and more environmentally sustainable catalytic methodologies.

Among many well-defined earth-abundant metal catalysts for alkene hydroboration that have emerged over the past decade, cobalt catalysts turned out to be most attractive with

respect to the ligand versatility, good regioselectivity of products and high TOFs.<sup>8–13</sup> Numerous cobalt catalyst systems have been reported for either branched (Markovnikov) or linear (anti-Markovnikov) selectivity by Chirik,<sup>9</sup> Lu,<sup>10</sup> Thomas,<sup>11</sup> Huang,<sup>12</sup> Findlater<sup>13</sup> and our group,<sup>8</sup> respectively. While all cobalt-based discrete molecular catalysts reported thus far realized alkene hydroboration with relatively low TOFs ( $<300\text{ h}^{-1}$ ), we have disclosed that a one-dimensional Co<sup>II</sup>-coordination polymer assembled from a divergent ligand, 4'-pyridyl-2,2'; 6',2''-terpyridine (pytpy), enabled Markovnikov-selective hydroboration of aryl alkenes with high TOFs up to  $47\,520\text{ h}^{-1}$ .<sup>8a</sup> However, the origin of the extremely high catalytic efficiency of this polymeric cobalt catalyst remained unclear. To better understand whether the polymeric structure of catalyst is vital for the unexpected activity, we decided to explore discrete molecular analogues of the polymeric precatalyst by using the same pytpy ligand and different cobalt salts (Scheme 1).

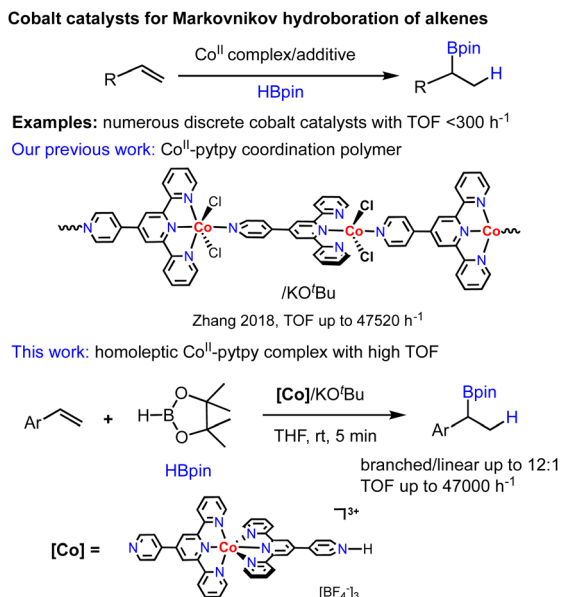
To continue our recent efforts on earth-abundant metal catalysis with tpy ligands,<sup>14</sup> herein, we report the synthesis and structural characterization of homoleptic octahedral Co<sup>II</sup> and Fe<sup>II</sup> complexes of pytpy containing tetrafluoroborate or hexafluorophosphate counterions (Scheme 2), and their surprisingly high catalytic activity for regioselective hydroboration of alkenes with high TOFs. Although homoleptic octahedral metal complexes of tpy derivatives have been well explored for electrochemical and photophysical properties, and some have been

<sup>a</sup>Department of Sciences, John Jay College and PhD Program in Chemistry, The Graduate Center of the City University of New York, New York, 10019 NY, USA. E-mail: [guzhang@jjay.cuny.edu](mailto:guzhang@jjay.cuny.edu)

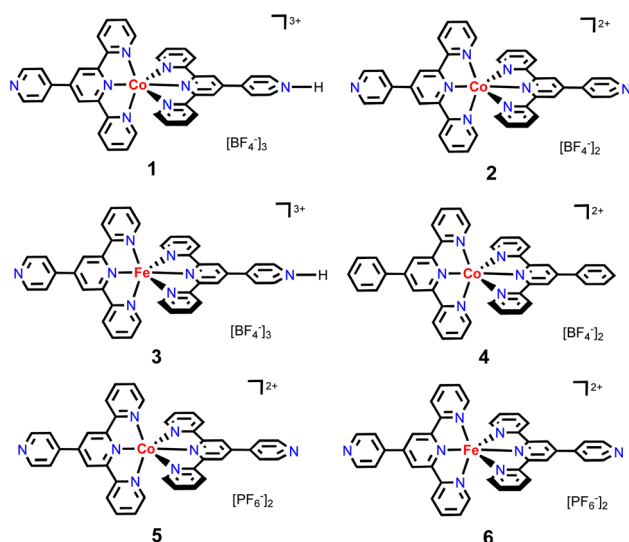
<sup>b</sup>Department of Chemistry, Hunter College, The City University of New York, New York, 10065 NY, USA

† Electronic supplementary information (ESI) available. CCDC 2284208–2284210. For ESI and crystallographic data in CIF or other electronic format see DOI: <https://doi.org/10.1039/d3ra06113b>





Scheme 1 The development of Co-catalysed hydroboration of alkenes.



Scheme 2 The structures of cobalt and iron complexes 1–6 studied in this work.

utilized as supramolecular synthons, they are considered to be less catalytically active as the coordination environment of the metal centers makes it relatively inaccessible during a catalytic event. Nevertheless, several examples of homoleptic Co, Fe and Ni tpy complexes have been reported to promote electrocatalytic reduction of CO<sub>2</sub>,<sup>15</sup> owing to their rich redox chemistry that can be tuned by varying electronic substituents on the tpy backbone.<sup>16</sup>

## Results and discussion

Carefully layering a solution of Co(BF<sub>4</sub>)<sub>2</sub>·6H<sub>2</sub>O in MeOH onto a CH<sub>2</sub>Cl<sub>2</sub>-MeOH solution (10 mL, 3 : 1, v/v) of pytpy over two

weeks led to the formation of red block-like crystals of **1** that were suitable for single-crystal X-ray diffraction analysis. A bulk sample of the crystals has been isolated in 92% yield. The solution <sup>1</sup>H NMR spectrum of **1** reveals broadened paramagnetic signals that could not be unambiguously assigned. The mass spectrum shows the only peak envelope at 679.1766 that can be assigned to the cation of the complex and the isotope pattern matches with that simulated. The solid-state structure of **1** was confirmed unambiguously by X-ray crystallography as a mono-protonated complex of [Co(pytpy)(H-pytpy)] [BF<sub>4</sub>]<sub>3</sub>, a product obtained serendipitously during attempts to produce the expected complex [Co(pytpy)<sub>2</sub>][BF<sub>4</sub>]<sub>2</sub>. **1** crystallizes in the monoclinic space group *P*2<sub>1</sub>/*c*. The spontaneous partial protonation of pytpy ligand during the complexation with transition metals is reminiscent of known Ru and Fe complexes of the same ligand.<sup>17,18</sup> The synthesis of **1** was well reproducible as evidenced from several independent layering experiments as well as the direct reaction between the ligand and Co(BF<sub>4</sub>)<sub>2</sub>·6H<sub>2</sub>O in a CH<sub>2</sub>Cl<sub>2</sub>-MeOH solution. In contrast, the originally expected homoleptic complex [Co(pytpy)<sub>2</sub>][BF<sub>4</sub>]<sub>2</sub> (**2**) has been synthesized by adopting the standard reaction sequence, *i.e.* the solution reaction of pytpy and CoCl<sub>2</sub>·6H<sub>2</sub>O followed by an anion exchange with excess amount of NaBF<sub>4</sub> (see ESI†). X-ray quality single crystals of **2** were obtained by vapor diffusion of diethyl ether into a solution of **2** in acetonitrile over 3 days. The mass spectrum of **2** shows the same peak envelope at 679.1766 as observed in **1**. X-ray structural analysis confirmed the structure of **2** as expected and it crystallizes in the monoclinic space group *Pc*. Co-crystallized solvent molecules of CH<sub>2</sub>Cl<sub>2</sub> and CH<sub>3</sub>CN were found in each cell of **1** and **2**, respectively.

The ORTEP representations of cations of **1** and **2** are shown in Fig. 1, respectively. In the cations of **1** and **2**, Co–N bond lengths around the cobalt coordination centers are within 1.8675(17)–2.1519(19) Å for **1** and 1.875(4)–2.182(4) Å for **2** (see caption of Fig. 1), which are unexceptional compared to the known crystal structures of Co(pytpy)<sub>2</sub>(PF<sub>6</sub>)<sub>2</sub> complexes.<sup>19</sup> The ligand conformations in **1** and **2** are not the same. In both structures, the non-coordinated pyridine ring is twisted with respect to the tpy domain to which it is attached. For **1**, the angles between the least squares planes of the rings containing atoms N2 and N4, and N6 and N8 are 33.32° and 34.84°, respectively. For **2**, the relevant twist angles are 40.36° and 34.71°. In addition, the deviation away from linearity of the N4⋯Co⋯N8 angle is notable for the cation of **1**. The angle of N4⋯Co⋯N8 is 167.73(2)° for the cation of **1**, but it is closer to linear in the cation of **2** (177.44(5)°). This is likely due to the ligand protonation in **1** and the resulting formation of one-dimensional (1-D) hydrogen-bonded chains as well as the major interchain π⋯π stacking between ‘side-arm’ pyridine rings observed in **1** (Fig. 2). A similar situation has been reported in relevant Fe and Ru complexes.<sup>17,18</sup> As seen in Fig. 2, the 1-D chain is assembled through N4–H4⋯N8(*i*) hydrogen bonds (symmetry code *i* = *x* – 1, *y*, *z* – 1, N4–H4 = 0.84(9) Å, H4⋯N8 = 1.82(9) Å, N4–H4⋯N8(*i*) = 172(7)°) and the chains are packed by π⋯π interaction of ‘side-arm’ pyridine rings (the closest C⋯C contact is 3.446(4) Å). Other types of π-stacking patterns are also observed in the 3-D packing framework of **1**. The intermolecular



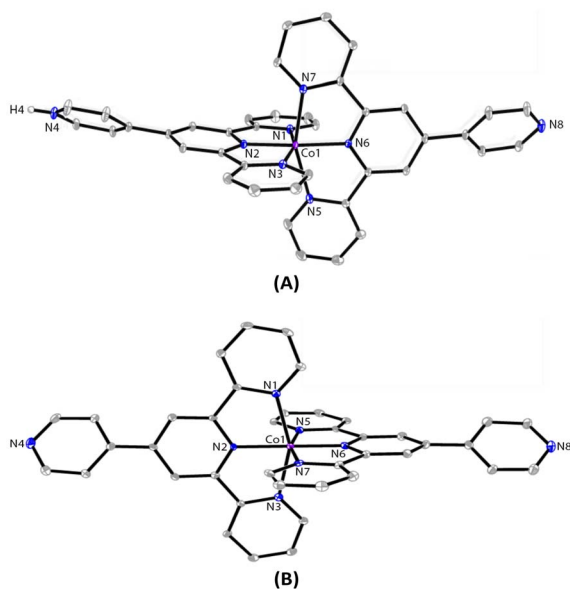


**Fig. 1** The ORTEP structures of **1** (A) and **2** (B) with thermal ellipsoids drawn at the 30% probability level.  $\text{BF}_4^-$  counterions and H atoms bound to C are omitted for clarity. Selected bond parameters for **1**: Co1–N1 = 1.998(2), Co1–N2 = 1.8675(17), Co1–N3 = 1.992(2), Co1–N5 = 2.150(2), Co1–N6 = 1.9270(18), Co1–N7 = 2.1519(19), N4–H4 = 0.84(9) Å, N1–Co1–N2 = 81.20(7), N2–Co1–N3 = 81.24(8), N5–Co1–N6 = 78.47(7), N6–Co1–N7 = 79.16(7)°; for **2**: Co1–N1 = 2.154(4), Co1–N2 = 1.943(4), Co1–N3 = 2.182(4), Co1–N5 = 1.989(4), Co1–N6 = 1.875(4), Co1–N7 = 1.987(4) Å, N1–Co1–N2 = 78.62(16), N2–Co1–N3 = 77.99(16), N5–Co1–N6 = 81.33(16), N6–Co1–N7 = 80.78(17)°.

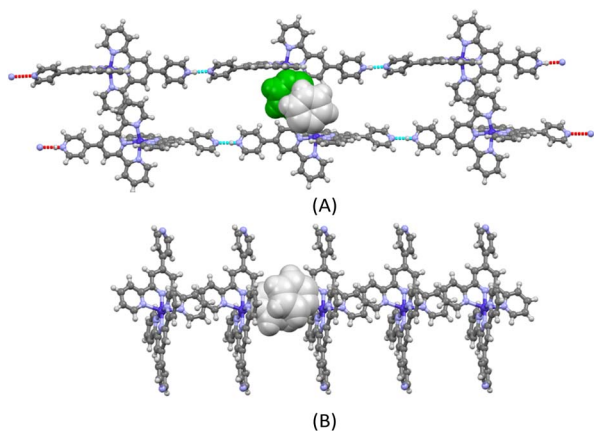


**Fig. 2** The 1-D hydrogen-bonded chains found in **1** and the  $\pi$ -stacking between the chains (A) and the intermolecular  $\pi$ -stacking in **2** (B).  $\text{BF}_4^-$  counterions and co-crystallized solvents are omitted for clarity.

packing in the cation of **2** is dominated by  $\pi \cdots \pi$  stacking between 'side-arm' pyridine rings (the closest C $\cdots$ C contact is 3.604(7) Å), similar to that of **1**.

Next, the reaction of pytpy with  $\text{Fe}(\text{BF}_4)_2 \cdot 6\text{H}_2\text{O}$  using the same layering method as for **1** resulted in the isolation of X-ray quality crystals of **3**. Complex **3** is isomorphic to **1** and also crystallizes in the monoclinic space group  $P2_1/c$ . A disordered solvent molecule in the asymmetric unit of **3** could not be well

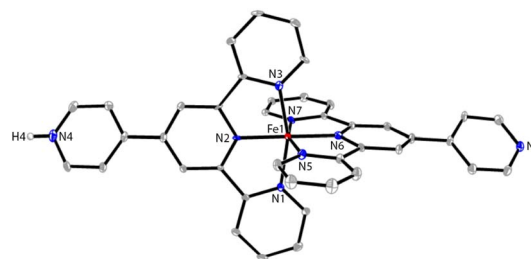


**Fig. 3** The ORTEP structure of **3** with thermal ellipsoids drawn at the 30% probability level.  $\text{BF}_4^-$  counterions and H atoms bound to C are omitted for clarity. Selected bond parameters: Fe1–N1 = 1.982(5), Fe1–N2 = 1.882(5), Fe1–N3 = 1.972(5), Fe1–N5 = 1.972(5), Fe1–N6 = 1.876(5), Fe1–N7 = 1.976(5), N4–H4 = 0.88(2) Å, N1–Fe1–N2 = 81.0(2), N2–Fe1–N3 = 81.2(2), N5–Fe1–N6 = 80.6(2), N6–Fe1–N7 = 81.2(2)°.

modelled and so it was treated as a diffuse contribution using PLATON/SQUEEZE.<sup>20</sup> The mono-protonated cation of **3** is shown in Fig. 3, which has been reported previously in compounds  $[\text{Fe}(\text{pytpy})(\text{pytpyH})][\text{Fe}(\text{NCS})_6] \cdot 2\text{H}_2\text{O}$  and  $[\text{Fe}(\text{pytpy})(\text{pytpyH})][\text{Fe}(\text{NCS})_6] \cdot \text{MeCN}$ .<sup>18</sup> The bending conformation in cation of **3** is very close to that found in **1** (angle  $\text{N4} \cdots \text{Fe1} \cdots \text{N8}$  is  $168.04(6)^\circ$ ), resulting from the intermolecular hydrogen bond  $\text{N4-H4} \cdots \text{N8}(i)$  (symmetry code  $i = x + 1, y, z + 1$ ,  $\text{N4-H4} = 0.88(2)$  Å,  $\text{H4} \cdots \text{N8} = 1.80(3)$  Å,  $\text{N4-H4} \cdots \text{N8}(i) = 167(8)^\circ$ ). Again, a similar 1-D hydrogen-bonded chain was found in **3**. As referenced, homoleptic complexes **4–6** (Scheme 2) were synthesized according to the procedure reported previously.<sup>21</sup>

In order to evaluate whether new octahedral  $\text{Co}^{\text{II}}$  and  $\text{Fe}^{\text{II}}$  complexes could be used as effective precatalysts for alkene hydroboration, we first adopted the optimized conditions as for  $[\text{Co}(\text{pytpy})\text{Cl}_2]_n$  to perform catalytic hydroboration of styrene with pinacolborane (HBpin). The results of catalytic screening are summarized in Table 1. To our delight, when **1** (0.025 mol%) and  $\text{KO}^t\text{Bu}$  (1 mol%) were combined in THF, the hydroboration of styrene was realized in 5 min to give the branched (**7**) and linear alkylboronates (**8**) in 98% total yield ( $\text{TOF} = \sim 47\,000 \text{ h}^{-1}$  for both regioisomers) and 9 : 1 regioselectivity (entry 1, Table 1), closely comparable to the results obtained by using polymeric  $[\text{Co}(\text{pytpy})\text{Cl}_2]_n$  as a precatalyst. This is remarkable and represents the first homoleptic octahedral cobalt(II) complex to enable alkene hydroboration with extremely high efficiency. Likewise, when **2** was used for the reaction under the same conditions, similar regioselectivity was found, while the yield dropped slightly to 80% ( $\text{TOF} = \sim 38\,000 \text{ h}^{-1}$ ). Interestingly, going from  $\text{Co}^{\text{II}}$  to  $\text{Fe}^{\text{II}}$  resulted in a notable loss of catalytic activity, as **3** catalysed the reaction with 17% yield in 5 min ( $8000 \text{ h}^{-1}$ ), although the regioselectivity remained (entry 3). In addition, both complexes **4** and **5** are moderately active precatalysts for styrene hydroboration (entries 4 and 5), indicating the importance of both the pytpy ligand and  $\text{BF}_4^-$  counterions for high catalytic efficiency. According to these results, it is not surprising to see that complex **6**,  $\text{Fe}(\text{pytpy})_2(\text{PF}_6)_2$ , is an inactive precatalyst (entry 6) under standard conditions.

Having established the ability of **1** as the best-performing precatalyst among six homoleptic complexes, we further screened the influence of reaction conditions such as solvents



Table 1 Condition screening for hydroboration of styrene with HBpin<sup>a</sup>

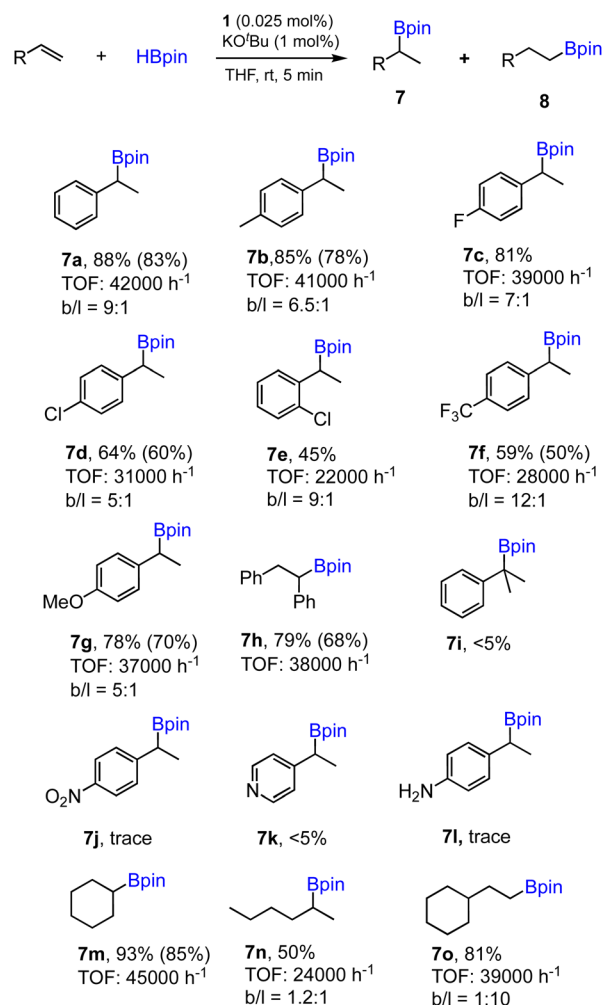
Entry	Precatalyst	Activator	Solvent	Yield <sup>b</sup> (%)	Ratio <sup>c</sup> (b/l)
1	1	KO <sup>t</sup> Bu	THF	98	9 : 1
2	2	KO <sup>t</sup> Bu	THF	80	8 : 1
3	3	KO <sup>t</sup> Bu	THF	17	10 : 1
4	4	KO <sup>t</sup> Bu	THF	35	8 : 1
5	5	KO <sup>t</sup> Bu	THF	41	9 : 1
6	6	KO <sup>t</sup> Bu	THF	<2	—
7	1	KO <sup>t</sup> Bu	Neat	50	3 : 1
8	1	KO <sup>t</sup> Bu	Toluene	<1	—
9	1	KO <sup>t</sup> Bu	CH <sub>2</sub> Cl <sub>2</sub>	2	—
10	1	KO <sup>t</sup> Bu	Et <sub>2</sub> O	62	9 : 1
11	1	KO <sup>t</sup> Bu	DMSO	58	5 : 1
12	1	NaO <sup>t</sup> Bu	THF	83	6 : 1
13	1	LiO <sup>t</sup> Bu	THF	20	3 : 1
14	1	KOCH <sub>3</sub>	THF	72	5 : 1
15	1	K <sub>2</sub> CO <sub>3</sub>	THF	59	8 : 1
16	1	LiNTf <sub>2</sub>	THF	2	—
17	1	NaHBET <sub>3</sub>	THF	88	5 : 1
18	—	KO <sup>t</sup> Bu	THF	0	—
19	1	—	THF	2	—
20	Co(BF <sub>4</sub> ) <sub>2</sub>	KO <sup>t</sup> Bu	THF	0	—
21 <sup>d</sup>	1	KO <sup>t</sup> Bu	THF	<5	—
22 <sup>e</sup>	1	KO <sup>t</sup> Bu	THF	97	9 : 1

<sup>a</sup> Conditions: styrene (1.0 mmol), HBpin (1.1 mmol), precatalyst (0.025 mol%), activator (1 mol%) and solvent (0.5 mL), 25 °C, 5 min, N<sub>2</sub>. <sup>b</sup> Yield of **7a** + **8a**, determined by GC analysis with hexamethylbenzene as an internal standard. <sup>c</sup> Ratio (b/l = **7a** : **8a**) determined by GC analysis. <sup>d</sup> Reaction run in the air. <sup>e</sup> Reaction run using 0.025 mol% of microcrystalline sample of **1**.

and activators on the catalytic performance. The solvent effect proved to be significant (entries 7–11). Much lower yield and regioselectivity were observed when the reaction was conducted without a solvent. Toluene and dichloromethane were incompatible solvents for this reaction, as only trace amount of product has been detected for reactions in these solvents. Diethyl ether and dimethylsulfoxide are relatively better, yet still inferior to THF in terms of yield and selectivity. Next, we examined the reaction with different activators (entries 12–17). The results suggest the key role played by KO<sup>t</sup>Bu as an activator for both high yield and regioselectivity, while other common activators such as NaO<sup>t</sup>Bu, K<sub>2</sub>CO<sub>3</sub> and NaHBET<sub>3</sub> all led to relatively poor results. Finally, control experiments were carried out to show that both cobalt complex and an activator are required to initiate the reaction (entries 18 and 19). It is also worth noting that when Co(BF<sub>4</sub>)<sub>2</sub> was used instead complex **1** as a precatalyst, no hydroboration of styrene was detected (entry 20). Under the optimal conditions with **1**/KO<sup>t</sup>Bu as catalyst, the reaction did not proceed when it was exposed to the air, indicating that a highly air-sensitive reactive intermediate (likely a cobalt hydride species) must have formed and was responsible for the high-efficiency catalysis (entry 21). It is worth mentioning that to achieve the high TOF and regioselectivity, a single crystalline

sample was not necessary. Instead, microcrystalline material of **1** could be synthesized in a gram-scale within 1–2 h by simply mixing concentrated, equimolar solutions of pytpy and Co(BF<sub>4</sub>)<sub>2</sub>·6H<sub>2</sub>O in CH<sub>2</sub>Cl<sub>2</sub> and MeOH, respectively (see the ESI<sup>†</sup>), and the hydroboration of styrene using this microcrystalline sample was found to be equally efficient (entry 22).

To further demonstrate the effectiveness of **1** as a precatalyst for other alkene substrates, we employed the optimized conditions (entry 1, Table 1) to examine substituted and functionalized styrenes. The results for a range of substrates tested are summarized in Scheme 3. First, methyl- and fluoro-substituted styrenes are suitable substrates affording the corresponding alkylboronates with high TOFs and slightly lower regioselectivity. Product **7b** was readily isolated from the mixture with 80% yield. However, when 4-chloro- or 2-chlorostyrene was used, the reaction ran slower and moderate yields were obtained in 5 min for both cases. Lower TOF (28 000 h<sup>-1</sup>) was also

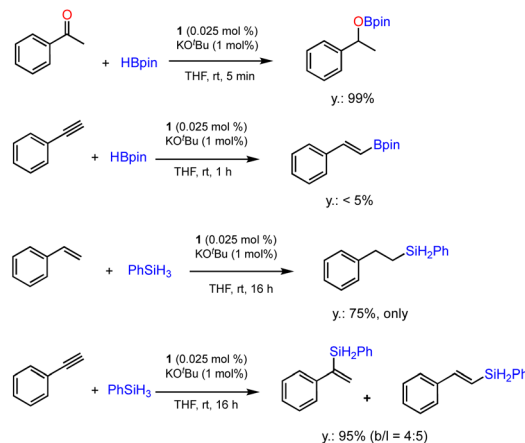


Scheme 3 Substrate scope for the hydroboration of alkenes using **1**/KO<sup>t</sup>Bu. Conditions: alkene (1.0 mmol), HBpin (1.1 mmol), **1** (0.025 mol%), KO<sup>t</sup>Bu (1 mol%) and THF (0.5 mL), 25 °C, 5 min, N<sub>2</sub>. Yields of products **7** and the ratio **7/8** (b/l) determined by GC analysis with hexamethylbenzene as an internal standard. TOF determined based on the yield of regioisomer **7** only. Yields of isolated products given in parentheses.



found in the case of 4-trifluoromethylstyrene as a substrate. Styrene with an electron-donating 4-methoxy group proceeded well with good yield, while the regioselectivity dropped to 5 : 1 (7g). *cis*-Stilbene was found to be active substrate for hydroboration to afford 7h with appreciable isolated yield and high TOF. However, 1,1-disubstituted alkene shows poor reactivity under standard conditions (7i). Styrenes containing functional groups such as nitro, amino or pyridyl are inactive substrates, similar to the results reported previously using polymeric [Co(pytpy)Cl<sub>2</sub>]<sub>n</sub> as a precatalyst.<sup>8a</sup> In addition, aliphatic and cyclic alkenes are also reactive substrates, however, poor regioselectivity was obtained for 1-hexene (7n) and anti-Markovnikov selectivity was found for vinylcyclohexane (7o).

Next, we explored the functional group tolerance of 1/KO<sup>t</sup>Bu system for styrene hydroboration by adding a second reducible substrate, which is so called a fast catalyst robustness screening.<sup>22</sup> Thus, styrene was chosen to react with HBpin under standard conditions in the presence of equimolar additives as listed in Table 2. Both ketone and aldehyde showed strongly competing reactions with styrene, as 60% ketone and 95% aldehyde hydroboration was detected as the major reactions, respectively (entries 1 and 2, Table 2). The ester showed little influence on the efficiency of styrene hydroboration with



**Scheme 4** Additional catalytic tests for hydroboration and hydrosilylation reactions using **1**. Conditions: substrate (0.5 mmol), HBpin or PhSiH<sub>3</sub> (0.55 mmol), **1** (0.025 mol%), KO<sup>t</sup>Bu (1 mol%) and THF (0.5 mL), 25 °C, N<sub>2</sub>, indicated time. Yields and regioselectivity determined by GC analysis using hexamethylbenzene as an internal standard.

**Table 2** Catalyst robust screening experiments<sup>a</sup>

Entry	Additive	Yield (7a + 8a) <sup>b</sup> /%	Ratio (7a/8a) <sup>b</sup>
1 <sup>c</sup>		40%	8 : 1
2 <sup>d</sup>		4%	—
3		72%	9 : 1
4		6%	—
5		3%	—
6		90%	15 : 1
7		35%	9 : 1

<sup>a</sup> Conditions: styrene (0.5 mmol), HBpin (0.5 mmol), **1** (0.025 mol%), KO<sup>t</sup>Bu (1 mol%), other reducible substrate (0.5 mmol) and THF (1 mL), 25 °C, 5 min, N<sub>2</sub>. <sup>b</sup> Determined by GC analysis using hexamethylbenzene as an internal standard. <sup>c</sup> 60% ketone hydroboration was detected. <sup>d</sup> 95% aldehyde hydroboration was detected.

no change on the regioselectivity (entry 3). However, both amide and nitrobenzene have completely suppressed the reactions (entries 4 and 5). Interestingly, butyronitrile is compatible with the reaction, while increasing the regioselectivity to 15 : 1 (entry 6). Finally, the presence of styrene oxide significantly decreased the yield of **7** albeit the regioselectivity remained. These results indicate somewhat inferior functional group tolerance of homoleptic complex **1**, compared to the polymeric precatalyst [Co(pytpy)Cl<sub>2</sub>]<sub>n</sub>.<sup>8a,14</sup>

The ability of precatalyst **1** to promote hydroboration and hydrosilylation for several other substrates was further evaluated. The preliminary results are presented in Scheme 4. The hydroboration of ketone was furnished under the standard conditions within 5 min, while phenylacetylene is almost inactive for hydroboration after 1 h. This is in sharp contrast with the results obtained using [Co(pytpy)Cl<sub>2</sub>]<sub>n</sub> as precatalyst where very high TOFs could be achieved.<sup>14b</sup> In addition, hydrosilylation of styrene and phenylacetylene using phenylsilane as a Si–H source has been investigated. It was found that styrene has experienced effective hydrosilylation to afford the anti-Markovnikov product with complete regioselective control. However, hydrosilylation of phenylacetylene was accomplished within 16 h in 95% yield with poor regioselectivity (*b/l* = 4 : 5). The results indicate that both reactivity and regioselectivity are highly substrate-dependent when using **1**/KO<sup>t</sup>Bu as the catalyst.

## Conclusions

In summary, we have synthesized and characterized homoleptic complexes of cobalt or iron with pytpy ligand. The direct reaction of pytpy and metal tetrafluoroborate resulted in the monoprotonation at the non-coordinating pyridyl moiety, namely [M(pytpy)(H-pytpy)][BF<sub>4</sub>]<sub>3</sub> (M = Co or Fe). X-ray structural analysis reveals the conformational bending of these complexes in the solid state due to the formation of 1-D hydrogen-bonded chains, in comparison with the common complex, Co(pytpy)<sub>2</sub>(BF<sub>4</sub>)<sub>2</sub>. These new complexes (**1–3**) along



with several known analogues (4–6) have been explored as precatalysts for the regioselective hydroboration of alkenes. The best catalytic system 1/KO<sup>t</sup>Bu was found to furnish the hydroboration of styrene with a very high TOF of  $\sim 47\,000\text{ h}^{-1}$ , comparable to the most efficient precatalyst [Co(pytpy)Cl<sub>2</sub>]<sub>n</sub> reported thus far. The method can be applied to a range of styrene derivatives for the regioselective synthesis of branched alkylboronates. However, some limitation of substrates has been disclosed. Catalyst robustness screening experiments provide further insights into the functional group tolerance of current catalyst. Preliminary experiments on relevant substrates for hydroboration and hydrosilylation catalysis were also conducted to extend its applicability for other conversions.

## Experimental

### General

Unless specified otherwise, all reactions were carried out under a dry N<sub>2</sub> atmosphere using standard glovebox and Schlenk techniques. Anhydrous grade solvents and reagents used were obtained from Aldrich or Fisher Scientific and stored over 4 Å molecular sieves. All chemicals of analytical grade including the alkene substrates and additives are used as received from Alfa Aesar, Acros, TCI America or Fisher Scientific without further purification. FT-IR spectra were recorded on a Shimadzu 8400S instrument with solid samples under N<sub>2</sub> using a Golden Gate ATR accessory. Elemental analyses were performed by Midwest Microlab LLC in Indianapolis in the US. <sup>1</sup>H NMR and <sup>13</sup>C NMR spectra were obtained at room temperature on a Bruker AV 400, 500 or 600 MHz NMR spectrometer, with chemical shifts ( $\delta$ ) referenced to the residual solvent signal. HR-MS data were obtained on an Agilent 6550 QToF coupled to an Agilent 1290 Infinity LC system. GC-MS analysis was obtained using a Shimadzu GCMS-QP2010S gas chromatograph mass spectrometer (column: SHR1-5MS, thickness: 0.25 m, diameter: 0.25 mm, length: 30.0 m; conditions: 30–200 °C, 10 °C min<sup>-1</sup>, injection temperature: 100 °C; solvent cutoff: 3 min).

### Synthesis of 1

A solution of pytpy (31.0 mg, 0.100 mmol) in MeOH/CH<sub>2</sub>Cl<sub>2</sub> (10 mL, 1 : 3, v/v) was placed in a test tube. A blank solution of MeOH/CH<sub>2</sub>Cl<sub>2</sub> (4 mL, 1 : 1, v/v) was layered on the top of the ligand solution, followed by a solution of Co(BF<sub>4</sub>)<sub>2</sub>·6H<sub>2</sub>O (34.1 mg, 0.100 mmol) in MeOH (8 mL). The tube was sealed and allowed to stand at room temperature for about four weeks, during which time X-ray quality yellow blocks grew at the bottom of the tube. The crystals were collected by decanting the solvent and washed with MeOH and then dried *in vacuo*. Yield: 43.2 mg (92% based on pytpy). FT-IR (solid, cm<sup>-1</sup>): 3078m, 1620m, 1597s, 1538s, 1470s, 1428s, 1405s, 1247s, 1031br, 822s, 786s, 733m. <sup>1</sup>H NMR (500 MHz, DMSO)  $\delta$  83.31 (bs), 48.22 (bs), 31.38 (bs), 30.84 (bs), 12.82 (bs), 10.49 (bs), 9.87 (bs) ppm. HR-MS (ESI positive): 679.1766 ([M-3(BF<sub>4</sub><sup>-</sup>)-H<sup>+</sup>], Cald. 679.1769). Anal. Calcd. for C<sub>40</sub>H<sub>29</sub>B<sub>3</sub>CoF<sub>12</sub>N<sub>8</sub>: C 51.05, H 3.11, N 11.91%. Found C 50.82, H 3.01, N 11.69. In a separate experiment, in a 100 mL flask, pytpy (0.62 g, 2.00 mmol) was dissolved in

MeOH/CH<sub>2</sub>Cl<sub>2</sub> (40 mL, 1 : 3, v/v), to which a solution of Co(BF<sub>4</sub>)<sub>2</sub>·6H<sub>2</sub>O (0.68 g, 2.00 mmol) in MeOH (20 mL) was added dropwise in 3 min. The reaction mixture was allowed to stay for an additional 1.5 h, red microcrystals had formed and were filtered to give bulk sample of 1 (yield: 0.83 g, 88%). Catalytic experiment confirmed its activity and efficiency for styrene hydroboration (entry 22, Table 1).

### Synthesis of 2

pytpy (31.0 mg, 0.100 mmol) was dissolved in MeOH/CH<sub>2</sub>Cl<sub>2</sub> (8 mL, 1 : 3, v/v) in a 20 mL vial, to which was added a solution of CoCl<sub>2</sub>·6H<sub>2</sub>O (11.9 mg, 0.050 mmol) in MeOH (3 mL). The mixture was stirred for 15 min at ambient temperature and then a solution of NaBF<sub>4</sub> (66.0 mg, 0.600 mmol) in MeOH (2 mL) was added, the resulting precipitate was filtered, washed with MeOH and dried *in vacuo*. X-ray quality crystals were obtained by slow diffusion of diethyl ether into a concentrated solution of 2 in acetonitrile. Yield: 34.5 mg (81%). FT-IR (solid, cm<sup>-1</sup>): 3057m, 1619m, 1597s, 1538s, 1470s, 1407s, 1245s, 1053br, 896m, 823m, 789s, 732m. <sup>1</sup>H NMR (400 MHz, DMSO)  $\delta$  83.42 (bs), 48.26 (bs), 31.69 (bs), 30.80 (bs), 12.82 (bs), 10.43 (bs), 9.92 (bs) ppm. HR-MS (ESI positive): 679.1766 ([M-2(BF<sub>4</sub><sup>-</sup>)], Cald. 679.1769). Anal. Calcd. for C<sub>40</sub>H<sub>28</sub>B<sub>2</sub>CoF<sub>8</sub>N<sub>8</sub>: C 56.31, H 3.31, N 13.13%. Found C 56.05, H 3.19, N 13.04.

### Synthesis of 3

The procedure is similar to that for 1, except that Fe(BF<sub>4</sub>)<sub>2</sub>·6H<sub>2</sub>O (33.8 mg, 0.100 mmol) was used. Brown plate-like crystals of 3 were collected in 85% yield (40 mg). FT-IR (solid, cm<sup>-1</sup>): 3603w, 3540w, 3075m, 1595s, 1537s, 1482m, 1467m, 1408s, 1286m, 1246m, 1053br, 895m, 821s, 788s, 755s, 733m. HR-MS (ESI positive): 676.1774 ([M-3(BF<sub>4</sub><sup>-</sup>)-H<sup>+</sup>], Cald. 676.1780).

### General procedure for 1-catalysed alkene hydroboration

In a glovebox under N<sub>2</sub> atmosphere, cobalt catalyst 1 (0.23 mg, 0.25  $\mu$ mol, 0.025 mol%) and KO<sup>t</sup>Bu (1.12 mg, 1 mol%) was dissolved in THF (0.5 mL) in a 3.8 mL glass vial equipped with a small stir bar. The mixture was stirred for 1 min. Alkenes (1.0 mmol) and pinacolborane (141 mg, 1.1 mmol) were then added. The reaction mixture was allowed to stir at room temperature for 5 min and then the reaction was quenched by exposing the reaction solution to air and adding CH<sub>2</sub>Cl<sub>2</sub> (1 mL) to the solution. The crude reaction mixture was first analyzed by GC-MS to determine the total yields of desired alkylboronates and the ratio of the regioisomeric products by comparing the GC traces with those of authentic samples.<sup>8a</sup> The reaction mixture for several selected products was then evaporated under reduced pressure and the product was purified through a SiO<sub>2</sub> column chromatography using ethyl acetate/hexane as an eluent. The pure alkylboronates of major products were characterized by <sup>1</sup>H and <sup>13</sup>C NMR spectroscopies.

### Catalyst robustness screening

In a glovebox under N<sub>2</sub> atmosphere, cobalt precatalyst 1 (0.12 mg, 0.025 mol%) and KO<sup>t</sup>Bu (1.12 mg, 1 mol%) was



dissolved in THF (0.5 mL) in a 3.8 mL glass vial equipped with a stir bar. The mixture was stirred for 1 min. Styrene (52 mg, 0.5 mmol), additive (0.5 mmol) and pinacolborane (64 mg, 0.5 mmol) were then added sequentially. Hexamethylbenzene (25 mg) was added as an internal standard for GC analysis. The reaction mixture was allowed to stir at room temperature for 5 min. The reaction was quenched by exposing the reaction solution to air and adding  $\text{CH}_2\text{Cl}_2$  (1 mL) to the solution. The crude product was analyzed by GC-MS to determine the GC yield and ratio of the regioisomeric products from styrene hydroboration. In each case, the identification of the corresponding boronate esters have been made by comparing their GC retention time and MS data with the authentic samples.<sup>8a</sup>

### X-ray crystallography

X-ray diffraction data were collected on a Bruker X8 Kappa Apex II diffractometer using Mo  $K\alpha$  radiation (for **1**) or on a Bruker D8 VENTURE diffractometer using Cu  $K\alpha$  radiation (for **2** and **3**). Crystal data, data collection and refinement parameters are summarized in Table S1 (ESI<sup>†</sup>). The structures were solved using a dual-space method and standard difference map techniques and were refined by full-matrix least-squares procedures on  $F^2$  with SHELXTL.<sup>23</sup> All hydrogen atoms bound to carbon were placed in calculated positions and refined with a riding model [ $U_{\text{iso}}(\text{H}) = 1.2 - 1.5U_{\text{eq}}(\text{C})$ ]. The hydrogen atom bound to nitrogen was located on the difference map and refined freely or with an N–H distance restraint (for **3**) [ $U_{\text{iso}}(\text{H}) = 1.2U_{\text{eq}}(\text{N})$ ].

### Author contributions

G. Z. and S. Z. conceived and supervised the project. H. Z., N. Z. and C. M. performed experimental studies. M. C. N. conducted the X-ray crystallographic analysis. All authors analysed the data and wrote the article.

### Conflicts of interest

There are no conflicts to declare.

### Acknowledgements

We are grateful to the financial support from the National Science Foundation (CHE #1900500 and #2247728) for this work. We also acknowledge the PSC-CUNY awards (65203-0053 and 66076-0054), the Seed grant from the Office for Advancement of Research and the PRISM program at John Jay College, the City University of New York. The X-ray diffractometer used for **2** and **3** was provided by the Air Force Office of Scientific Research under award number FA9550-20-1-0158.

### Notes and references

- (a) B. T. Cho, *Chem. Soc. Rev.*, 2009, **38**, 443–452; (b) A. Togni and H. Grützmacher, *Catalytic Hydrofunctionalization*, Wiley-VCH, Weinheim, 2001; (c) M. B. Smith and J. March, *March's Advanced Organic Chemistry*, Wiley-Interscience, Hoboken, NJ, 6th edn, 2007, pp. 1703–1869; (d)

*Hydrofunctionalization*, Topics in Organometallic Chemistry, ed. V. P. Ananikov and M. Tanaka, Springer-Verlag, Berlin, Heidelberg, 2013, p. 43.

- A. Singh, S. Shafiei-Haghighi, C. R. Smith, D. K. Unruh and M. Findlater, *Asian J. Org. Chem.*, 2020, **9**, 416–420.
- (a) K. Burgess and M. J. Ohlmeyer, *Transition-Metal Promoted Hydroborations of Alkenes, Emerging Methodology for Organic Transformations*, *Chem. Rev.*, 1991, **91**, 1179–1191; (b) C. M. Crudden and D. Edwards, *Catalytic Asymmetric Hydroboration: Recent Advances and Applications in Carbon–Carbon Bond-Forming Reactions*, *Eur. J. Org. Chem.*, 2003, **2003**, 4695–4712; (c) Y. Yamamoto, R. Fujikawa, T. Umemoto and N. Miyaura, *Iridium-Catalyzed Hydroboration of Alkenes with Pinacolborane*, *Tetrahedron*, 2004, **60**, 10695–10700; (d) A. M. Carroll, T. P. O'Sullivan and P. J. Guiry, *The Development of Enantioselective Rhodium-Catalysed Hydroboration of Olefins*, *Adv. Synth. Catal.*, 2005, **347**, 609–631; (e) C. M. Vogels and S. W. Westcott, *Recent Advances in Organic Synthesis Using Transition Metal-Catalyzed Hydroborations*, *Curr. Org. Chem.*, 2005, **9**, 687–699; (f) D. R. Edwards, Y. B. Hleba, C. J. Lata, L. A. Calhoun and C. M. Crudden, *Regioselectivity of the Rhodium-Catalyzed Hydroboration of Vinyl Arenes: Electronic Twists and Mechanistic Shifts*, *Angew. Chem., Int. Ed.*, 2007, **46**, 7799–7802; (g) S. Kisan, V. Krishnakumar and C. Gunanathan, *Ruthenium-Catalyzed Anti-Markovnikov Selective Hydroboration of Olefins*, *ACS Catal.*, 2017, **7**, 5950–5954; (h) G. Wang, X. Liang, L. Chen, Q. Gao, J. G. Wang, P. Zhang, Q. Peng and S. Xu, *Iridium-Catalyzed Distal Hydroboration of Aliphatic Internal Alkenes*, *Angew. Chem., Int. Ed.*, 2019, **58**, 8187–8191.
- (a) J. V. Obligation and P. J. Chirik, *Earth-Abundant Transition Metal Catalysts for Alkene Hydrosilylation and Hydroboration: Opportunities and Assessments*, *Nat. Rev. Chem.*, 2018, **2**, 15–34; (b) M. D. Greenhalgh, A. S. Jones and S. P. Thomas, *Iron-Catalysed Hydrofunctionalisation of Alkenes and Alkynes*, *ChemCatChem*, 2015, **7**, 190–222; (c) H. Wen, G. Liu and Z. Huang, *Recent advances in tridentate iron and cobalt complexes for alkene and alkyne hydrofunctionalizations*, *Coord. Chem. Rev.*, 2019, **386**, 138–153; (d) W. Fan, L. Li and G. Zhang, *Branched-selective alkene hydroboration catalyzed by earth-abundant metals*, *J. Org. Chem.*, 2019, **84**, 5987–5996; (e) S. R. Tamang and M. Findlater, *Emergence and Applications of Base Metals (Fe, Co, and Ni) in Hydroboration and Hydrosilylation*, *Molecules*, 2021, **24**, 319; (f) J. Guo, Z. Cheng, J. Chen, X. Chen and Z. Lu, *Iron- and cobalt-catalyzed asymmetric hydrofunctionalization of alkenes and alkynes*, *Acc. Chem. Res.*, 2021, **54**, 2701–2716.
- C. Li, S. Song, Y. Li, C. Xu, Q. Luo, Y. Guo and X. Wang, *Selective hydroboration of unsaturated bonds by an easily accessible heterotopic cobalt catalyst*, *Nat. Commun.*, 2021, **12**, 3813.
- M. Zhong, Y. Gagné, T. O. Hope, X. Pannecoucke, M. Frenette, P. Jubault and T. Poisson,



- Copper-Photocatalyzed Hydroboration of Alkynes and Alkenes, *Angew. Chem., Int. Ed.*, 2021, **133**, 14619–14624.
- 7 G. Zhang, H. Zeng, J. Wu, Z. Yin, S. Zheng and J. C. Fettinger, Highly Selective Hydroboration of Alkenes, Ketones and Aldehydes Catalyzed by a Well-Defined Manganese Complex, *Angew. Chem., Int. Ed.*, 2016, **55**, 14369–14372.
- 8 (a) G. Zhang, J. Wu, S. Li, S. Cass and S. Zheng, Markovnikov-Selective Hydroboration of Vinylarenes Catalyzed by a Cobalt (II) Coordination Polymer, *Org. Lett.*, 2018, **20**, 7893–7897; (b) G. Zhang, J. Wu, M. Wang, H. Zeng, J. Cheng, M. C. Neary and S. Zheng, Cobalt-Catalyzed Regioselective Hydroboration of Terminal Alkenes, *Eur. J. Org. Chem.*, 2017, **2017**, 5814–5818.
- 9 W. N. Palmer, T. Diao, I. Pappas and P. J. Chirik, High-Activity Cobalt Catalysts for Alkene Hydroboration with Electronically Responsive Terpyridine and  $\alpha$ -Diimine Ligands, *ACS Catal.*, 2015, **5**, 622–626.
- 10 X. Chen, Z. Cheng and Z. Lu, Cobalt-Catalyzed Asymmetric Markovnikov Hydroboration of Styrenes, *ACS Catal.*, 2019, **9**, 4025–4029.
- 11 J. Peng, J. H. Docherty, A. P. Dominey and S. P. Thomas, Cobalt-Catalysed Markovnikov Selective Hydroboration of Vinylarenes, *Chem. Commun.*, 2017, **53**, 4726–4729.
- 12 J. Liu, J. Du, F. Yu, L. Gan, G. Liu and Z. Huang, Thermally Robust and Highly Active PCP Cobalt (II) Catalyst for Linear-Selective Hydroboration of Terminal and Internal Olefins, *ACS Catal.*, 2023, **13**, 7995–8003.
- 13 S. R. Tamang, D. Bedi, S. Shafiei-Haghighi, C. R. Smith, C. Crawford and M. Findlater, Cobalt-catalyzed hydroboration of alkenes, aldehydes, and ketones, *Org. Lett.*, 2018, **20**, 6695–6700.
- 14 (a) J. Wu, H. S. Zeng, J. Cheng, S. P. Zheng, J. A. Golen, D. R. Manke and G. Zhang, *J. Org. Chem.*, 2018, **83**, 9442–9448; (b) G. Zhang, S. Li, J. Wu, H. Zeng, Z. Mo, K. Davis and S. Zheng, *Org. Chem. Front.*, 2019, **6**, 3228–3233; (c) G. Zhang, J. Wu, H. Zeng, M. C. Neary, M. Devany, S. Zheng and P. A. Dub, *ACS Catal.*, 2019, **9**, 874–884; (d) G. Zhang, J. Wu, S. Zheng, M. C. Neary, J. Mao, M. Flores, R. J. Trovitch and P. A. Dub, *J. Am. Chem. Soc.*, 2019, **141**, 15230–15239; (e) G. Zhang, J. Cheng, K. Davis, M. G. Bonifacio and C. Zajaczkowski, *Green Chem.*, 2019, **21**, 1114–1121; (f) G. Zhang, H. Zeng, S. Zheng, M. C. Neary and P. A. Dub, Vanadium-Catalyzed Stereo- and Regioselective Hydroboration of Alkynes to Vinyl Boronates, *ACS Catal.*, 2022, **12**, 5425–5429; (g) G. Zhang, S. Zheng and M. C. Neary, An ionic Fe-based metal-organic-framework with 4'-pyridyl-2,2':6',2''-terpyridine for catalytic hydroboration of alkynes, *RSC Adv.*, 2023, **13**, 2225–2232.
- 15 (a) N. Elgrishi, M. B. Chambers, V. Artero and M. Fontecave, Terpyridine complexes of first row transition metals and electrochemical reduction of CO<sub>2</sub> to CO, *Phys. Chem. Chem. Phys.*, 2014, **16**, 13635–13644; (b) S. Suhr, N. Schröter, M. Kleoff, N. Neuman, D. Hunger, R. Walter, C. Lücke, F. Stein, S. Demeshko, H. Liu and H. U. Reissig, Spin State in Homoleptic Iron (II) Terpyridine Complexes Influences Mixed Valency and Electrocatalytic CO<sub>2</sub> Reduction, *Inorg. Chem.*, 2023, **62**, 6375–6386.
- 16 J. C. Dickenson, M. E. Haley, J. T. Hyde, Z. M. Reid, T. J. Tarring, D. A. Iovan and D. P. Harrison, Fine-tuning metal and ligand-centered redox potentials of homoleptic bis-terpyridine complexes with 4'-aryl substituents, *Inorg. Chem.*, 2021, **60**, 9956–9969.
- 17 J. E. Beves, D. J. Bray, J. K. Clegg, E. C. Constable, C. E. Housecroft, K. A. Jolliffe, C. J. Kepert, L. F. Lindoy, M. Neuburger, D. J. Price and S. Schaffner, Expanding the 4, 4'-bipyridine ligand: Structural variation in {M(pytpy)<sub>2</sub>}<sup>2+</sup> complexes (pytpy= 4'-(4-pyridyl)-2,2':6',2''-terpyridine, M= Fe, Ni, Ru) and assembly of the hydrogen-bonded, one-dimensional polymer {[Ru(pytpy)(Hpytpy)]<sub>n</sub>}<sup>3n+</sup>, *Inorg. Chim. Acta*, 2008, **361**, 2582–2590.
- 18 J. E. Beves, E. C. Constable, C. E. Housecroft, C. J. Kepert, M. Neuburger, D. J. Price and S. Schaffner, The conjugate acid of bis {4'-(4-pyridyl)-2,2':6',2''-terpyridine} iron (II) as a self-complementary hydrogen-bonded building block, *CrystEngComm*, 2007, **9**, 1073–1077.
- 19 Y. Guo, X. L. Yang, R. J. Wei, L. S. Zheng and J. Tao, Spin transition and structural transformation in a mononuclear Cobalt (II) complex, *Inorg. Chem.*, 2015, **54**, 7670–7672.
- 20 (a) A. L. Spek, *PLATON, A Multipurpose Crystallographic Tool*, Utrecht University, Utrecht, The Netherlands, 2005; (b) A. L. Spek, Single-crystal structure validation with the program PLATON, *J. Appl. Crystallogr.*, 2003, **36**, 7–13.
- 21 (a) E. C. Constable, J. Lewis, M. C. Liptrot and P. R. Raithby, The coordination chemistry of 4'-phenyl-2, 2': 6', 2''-terpyridine; the synthesis, crystal and molecular structures of 4'-phenyl-2,2':6',2''-terpyridine and bis (4'-phenyl-2,2':6',2''-terpyridine) nickel (II) chloride decahydrate, *Inorg. Chim. Acta*, 1990, **178**, 47–54; (b) J. E. Beves, E. L. Dunphy, E. C. Constable, C. E. Housecroft, C. J. Kepert, M. Neuburger, D. J. Price and S. Schaffner, Vectorial property dependence in bis {4'-(n-pyridyl)-2,2':6',2''-terpyridine} iron (ii) and ruthenium (ii) complexes with n= 2, 3 and 4, *Dalton Trans.*, 2008, **3**, 386–396; (c) P. C. Mondal, V. Singh and B. Shankar, Ferropyridyl complex based multiple switches for application in molecular logic gates and circuits, *New J. Chem.*, 2014, **38**, 2679–2685.
- 22 K. D. Collins and F. A. Glorius, Robustness Screen for the Rapid Assessment of Chemical Reactions, *Nat. Chem.*, 2013, **5**, 597–601.
- 23 (a) G. M. Sheldrick, *SHELXTL, An Integrated System for Solving, Refining, and Displaying Crystal Structures from Diffraction Data*, University of Göttingen, Göttingen, Federal Republic of Germany, 1981; (b) G. M. Sheldrick, SHELXT-Integrated Space-Group and Crystal-Structure Determination, *Acta Crystallogr.*, 2015, **A71**, 3–8.

